Biochemistry and Biophysics Reports 28 (2021) 101105

Contents lists available at ScienceDirect

Biochemistry and Biophysics Reports

journal homepage: www.elsevier.com/locate/bbrep

Identification of genetic modifiers of murine hepatic β-glucocerebrosidase activity

Anyelo Durán [a,1], Boris Rebolledo-Jaramillo [a,1], Valeria Olguin [a], Marcelo Rojas-Herrera [a], Macarena Las Heras [a], Juan F. Calderón [a], Silvana Zanlungo [b], David A. Priestman [c], Frances M. Platt [c], Andrés D. Klein [a,*]

[a] Centro de Genética y Genómica, Facultad de Medicina, Clínica Alemana, Universidad del Desarrollo, Santiago, Chile
[b] Department of Gastroenterology, Faculty of Medicine, Pontificia Universidad Católica de Chile, Santiago, Chile
[c] Department of Pharmacology, University of Oxford, Oxford, OX1 3QT, UK

ARTICLE INFO

Keywords:
Systems genetics
Modifier genes
β-glucocerebrosidase
Inbred strains
Gaucher disease
Parkinson's disease

ABSTRACT

The acid β-glucocerebrosidase (GCase) enzyme cleaves glucosylceramide into glucose and ceramide. Loss of function variants in the gene encoding for GCase can lead to Gaucher disease and Parkinson's disease. Therapeutic strategies aimed at increasing GCase activity by targeting a modulating factor are attractive and poorly explored. To identify genetic modifiers, we measured hepatic GCase activity in 27 inbred mouse strains. A genome-wide association study (GWAS) using GCase activity as a trait identified several candidate modifier genes, including *Dmrtc2* and *Arhgef1* ($p=2.1x10^{-7}$), and *Grik5* ($p=2.1x10^{-7}$). Bayesian integration of the gene mapping with transcriptomics was used to build integrative networks. The analysis uncovered additional candidate GCase regulators, highlighting modules of the acute phase response ($p=1.01x10^{-8}$), acute inflammatory response ($p=1.01x10^{-8}$), fatty acid beta-oxidation ($p=7.43x10^{-5}$), among others. Our study revealed previously unknown candidate modulators of GCase activity, which may facilitate the design of therapies for diseases with GCase dysfunction.

1. Introduction

Hydrolytic enzymes are abundant in the lysosome; more than 60 acidic hydrolases have been described to date [1]. In addition to its digestive and recycling functions, the lysosome orchestrates metabolic adaptations to external cues [2]. The acidic lysosomal β-glucocerebrosidase (GCase) enzyme degrades glucosylceramide into glucose and ceramide [3]. GCase is encoded by the *GBA1* gene. Loss-of-function variants in this gene cause the rare lysosomal storage disorder Gaucher disease (GD) [4]. *GBA1* variants also significantly increase the risk of developing Parkinsonism and Parkinson's disease (PD) [5]. In addition to other mechanistic data, this observation highlights the role of lysosomal dysfunction as a risk factor for PD [6]. Therefore, an exogenous increase of GCase activity and other related enzymes is an attractive therapeutic strategy that has not yet been thoroughly explored.

Although treatments for Gaucher disease are available, they have clinical limitations [7]. Studying how GCase is modulated can allow us to i) learn about its regulation and possibly ii) develop new targeted therapies to treat these diseases which diseases be more specific. One attractive approach to identify new therapeutic targets to modulate GCase is to use the natural genetic diversity present in populations of individuals (i.e., model organisms) to identify genetic modifiers that control a given trait [8]. By integrating gene mapping with other sets of -omics, it is possible to find regulatory elements underlying the variation in a given trait [9]. This holistic population-based approach is called systems genetics [10].

Inbred mouse strains arise from crossing siblings for at least 20 generations [11]. The Hybrid Mouse Diversity Panel (HMDP) [8] corresponds to a panel of genotyped inbred strains where other -omics data are also available [8,12]. The HMDP panel has been used to perform association studies and find modifier genes for a variety of complex traits [13,14].

Here, we used a systems genetics approach to identify putative

* Corresponding author. Av. Las Condes 12.461, Postal Zip code 7590943, Santiago, Chile.
E-mail address: andresklein@udd.cl (A.D. Klein).
[1] Equal contribution.

https://doi.org/10.1016/j.bbrep.2021.101105
Received 4 June 2021; Received in revised form 11 August 2021; Accepted 12 August 2021
Available online 18 August 2021

modifier genes/networks of GCase activity in mice. To this end, we measured hepatic GCase activity in 27 strains of mice. A genome-wide association (GWAS) analysis identified putative modifier genes. We used Mergeomics analysis to integrate GCase activity, gene mapping, and available liver transcriptomic data. Our study revealed genes, networks, and biological processes that might regulate GCase function.

2. Materials and methods

2.1. Mouse tissues

We used 8 weeks-old mice livers derived from 27 inbred mouse strains which were kindly donated by Dr. Aldons Lusis (University of California, Los Angeles). (i) 129X1/SvJ (n=5), (ii) A/J (n=5), (iii) AKR/J (n=5), (iv) BALB/cJ (n=5), (v) BTBR T<+> tf/J (n=5), (vi) BUB/BnJ (n=3), (vii) C3H/HeJ (n=3), (viii) C57BL/6J (n=5), (ix) C58/J (n=5), (x) CAST/EiJ (n=3), (xi) CBA/J (n=5), (xii) CE/J (n=5), (xiii) DBA/2J (n=5), (xiv) FVB/NJ (n=3), (xv) KK/HlJ (n=3), (xvi) LG/J (n=4), (xvii) LP/J (n=3), (xviii) MA/MyJ (n=3), (xix) NOD/ShiLtJ (n=5), (xx) NON/ShiLtJ (n=5), (xxi) NZB/BlNJ (n=5), (xxii) NZW/LacJ (n=5), xxiii) PL/J (n=5), xxiv) RIIIS/J (n=3), xxv) SEA/GnJ (n=5), xxvi) SM/J (n=5), xxvii) SWR/J (n=5). Tissues were homogenized and adjusted to 50 mg tissue/ml in H_2O, with a Potter-Elvehjem tissue homogenizer (Omni International, USA) and then stored at −80 °C until further use. This liver was selected because of its high relevance in the generation of pathophysiological phenotypes in GD [4].

2.2. GCase activity assays

GCase activity was determined using an artificial fluorescent substrate based on 4-methylumbelliferone (4-MU) [15]. For this purpose, liver homogenates were diluted 1/10 with GCase buffer (200 mM citrate-phosphate buffer, pH 5.2, containing 0.25% Triton X-100, 1.25 mM EDTA, 4 mM 2-mercaptoethanol, all these reagents from Calbiochem, Merck KGaA, Darmstadt, Germany). Three cycles of freezing and thawing with liquid nitrogen were performed to disrupt the cell membranes. Subsequently, 10 μl of the diluted homogenates (5 μg of total protein from each sample) were mixed with and without 10 μl of 0.3 mM N-butyldeoxydeoxynojirimycin (NB-DGJ) for 30 min on ice. *N*B-DGJ is a β-glucocerebrosidase 2 (GBA2; non-lysosomal enzyme) inhibitor that does not inhibit GCase [16] (Toronto Research Chemicals, North York, Ontario, Canada). Thereafter, the tubes were placed in a 37 °C water bath, and 40 μl of the substrate 4-methylumbelliferyl-β-D-glucopyranoside (4.5 mM 4-MU-β-D-Glc in GCase buffer) (Sigma, Dorset, England) was added. The reaction was stopped after 30 min of incubation by the addition of 400 μl cold 0.5 M Na_2CO_3 at pH 10.7 (Panreac Applichem, Barcelona, Spain). Fluorescence was measured at 340 nm excitation and 460 nm emission with a gain of 40 in a semi-automated plate reader (Synergy HT, BioTek, Winooski, USA). Fluorescence values were normalized to protein content in each sample as obtained by a BSA assay (Pierce BCA Protein Assay Kit; Thermo Fisher Scientific, Illinois, USA). To calculate GCase specific activity, a 4-MU standard curve was constructed, and the final value was adjusted to 1 h of enzymatic reaction. For each biological sample, at least three technical replicates were performed.

2.3. Phylogenetic tree and GWAS using an efficient mixed model association (EMMA)

We used the average GCase activity per mouse strain as a phenotype to perform the GWAS using an Efficient Mixed Model Association Study (EMMA v.1.1.2) [17]. In addition, we included in the analysis the mouse HapMap reference panel, consisting of 4 million SNVs downloaded from http://mouse.cs.ucla.edu/mousehapmap/full.html [18]. The R package for EMMA was downloaded from http://mouse.cs.ucla.edu/emma/ [19]. P-value was recorded as the strength of the genotype-phenotype associations. To build to phylogenetic tree we used the EMMA uses a kinship matrix to run hierarchical clustering using R [19].

2.4. Gene expression array

The hepatic transcript levels of inbred mouse strains were downloaded from the repository GSE16780 UCLA Mouse MDP Liver Affy HT M430A MDP Liver [20]. If there was more than one probe quantifying the same gene, the values were averaged.

2.5. Functional impact of gene variants

We downloaded the genomes of three strains with low and high GCase activity respectively (CBA/J, A/J, FVB/NJ, CAST/EiJ, BUB/BnJ, and C58/J) from the Mouse Phenome Database (MPD) (RRID: SCR_003212) of Jackson Laboratory (https://phenome.jax.org/) and Mouse Genomes Project of Sanger Institute [21]. The Impact of variants was assessed using SIFT (sorting intolerant from tolerant) [22] and SnpEff [23].

2.6. Integrative networks of genomic and transcriptomic data

To study how genomic and liver transcriptomic variation contributes to hepatic GCase activity variability in the 27 HMDP strains, we employed Mergeomics v1.18 [24]. To build Bayesian networks of integrative omics underlying GCase activity, two modules of Mergeomics are required: a) marker set enrichment analysis (MSEA) and b) weighted key driver analysis (wKDA). MSEA requires the following data inputs: 1) EMMA GWAS results: i) marker-GCase activity association (marker--value) and ii) gene-marker mapping file (gene-marker); 2) functionally related gene sets (module-gene), which are preloaded in Mergeomics. These results are integrated through the package algorithm to find sets of genes associated with GCase activity. The parameter settings of the MSEA module included: i) type of permutation at the gene level. ii) minimum (10) and maximum (500) number of genes in the sets. iii) the minimum and maximum overlap ratio between sets of genes associated with disease/trait = 0.33 (33% overlap). iv) the number of gene or marker permutations = 2000 and finally v) the MSEA FDR cutoff was ≤25% [25], this analysis calculates the Benjamini-Hochberg FDR [26].

To identify key driver (KD) genes, which are defined as the gene hubs most significantly associated with other genes in the network, we used wKDA [24]. The wKDA module takes input data from the MSEA results generated in the previous step and a defined liver tissue Bayesian network corresponding to human and rodent expression datasets of earlier studies [27]. The parameters for running wKDA included i) Search depth of wKDA = 1, which means that we search for key-drivers whose immediate neighborhood is enriched for MSEA significant genes, ii) the edge type of wKDA = incoming and outgoing directionality, iii) the minimum overlap, is the threshold above which hubs will be designated as co-hubs, of wKDA = 0.33, and iv) the edge factor of wKDA = 0.5, which means an unweight network. This module projected sets of genes associated with liver GCase activity onto a Bayesian liver network, representing seemingly causal relationships between genes and KD genes [27]. We ran both Mergeomics modules in the R package [19].

2.7. Gene ontology enrichment

ShinyGO v0.61 [28], for gene ontology (GO) enrichment analysis for network modules, was employed. This tool has annotations for model organisms. The chromosomal gene location, metabolic pathways, gene clustering, and protein interaction networks can be plotted [28].

2.8. Statistics

Prism v9.1.0 (GraphPad software, San Diego, CA) and the R package [25] was used for statistical analysis and included a two-tailed Student's

t-test and ANOVA with Bonferroni test. Pearson for correlation analyses was employed. The significant value was considered as $p < 0.05$.

3. Results

3.1. Liver GCase activity varies among mouse strains

We measured hepatic GCase activity by fluorimetry in the liver of 27 inbred mice strains with different phylogenetic origins (Fig. 1A) using an artificial substrate 4-MU-β-D-Glc. We observe significant variability in the average enzymatic activity between the different strains (Fig. 1B). This activity was higher in the BUB/BnJ and C58/J strains ($p < 0.001$; mean ± 95%confidence interval; 39.3 ± 25.0–53.5 and 40.1 ± 29.57–50.6 respectively) compared to MA/MyJ and CBA/J (20.7 ± 10.3–31.2 and 23.8 ± 16.8–30.7 respectively).

3.2. GWAS identified putative modifier genes of GCase activity

To uncover possible modifier genes, we performed a GWAS analysis with EMMA. EMMA is a statistical test that corrects the strains' population structure and genetic relatedness. EMMA applies a mixed models for association mapping, allowing to substantially increase the computational speed and reliability of the results by reducing false positives associations [17]. We found 271 significant Single Nucleotide Variants (SNVs) $p \leq 4.1x10^{-6}$ that exceeded the threshold of suggestive associations previously established [36], represented in 9 non-redundant genes (Table S1 and Fig. 2A). Among all the variants identified, we found an exonic variant in the *Myo6* gene, one in the 3′UTR region of *Dmrtc2* and A*rhgef1*, among others (Table S1). Then, we organized the strains by GCase activity and plotted the genotypes of the top associated markers. The strains with low and intermediate activities present a different distribution pattern than those with high GCase activity (Fig. 2B). Strains AKR/J and PL/J showed a different distribution pattern. Perhaps in these two strains, spontaneous mutations arose in some of their generations after genotyping, as described for C3H/HeN, BL6, BALBc, and FVB [29]. A suggestive association threshold (blue line) (Fig. 2A) $p \leq 4.1x10^{-6}$ was calculated in Ref. [17,29] and ii) a Bonferroni correction, which resulted in a much stricter *p*-value of $1.28x10^{-8}$, denoted by the red line in Fig. 2A. Interestingly we observed variants at different genomic locations with a genotype-phenotype association that exceeds the empirical *p*-value (Fig. 2A &B).

3.3. Associations between hepatic transcripts levels and GCase enzyme activity

The significant SNVs in a GWAS can be regulators of gene expression levels. Thus, we performed correlation studies between GCase activity and liver transcripts levels. To this end, we downloaded the hepatic gene expression array data from an online repository (GSE16780 UCLA Mouse MDP Liver Affy HT M430A) [20]. The array included the probes for seven of the nine identified genes. Associations were explored (Fig. S1). No significant correlations were found. The array data that we used did not include probes for *Spag16* and *Dmrtc2* genes. Therefore, it was not possible to test correlations with these two genes. For *Erbb4* and *Zic4* we observed a trend (p=0.07). The signals in a Manhattan plot can be labeling coding or other no coding genomic variability. To explore this possibility, we downloaded the genomes of three low (CBA/J, A/J, and FVB/NJ) and three high (CAST/EiJ, BUB/BnJ, and C58/J) GCase activity strains from the Mouse Genomes Project of Sanger Institute [21]. We identified predicted splice and or miss sense variants in *Grik5*, *Impg1*, *Myo6*, and *Spag16* (Fig. 2C). To assess the implications of miss sense variants we used SIFT (sorting intolerant from tolerant) [22] and SnpEff [23].

3.4. Identification of modules, key drivers, and pathways associated with GCase activity

EMMA/GWAS results were used to identify modules and key driver genes within the coexpression network re-constructed for mouse/human liver, using Mergeomics v1.18. We used 20 pre-defined mouse gene sets [24] and FDR <25%. The MSEA module of Mergeomics highlighted modules which correspond to mouse liver expression data converted to human gene symbols (Table S2). The wKDA identified 4 top key drivers (*Itih4, Hsd3b5, Ocel1, Pigt*) and 18 total network hubs (Fig. 3A, Table S2). We included the significant correlations between GCase activity, and the transcripts identified in the network (Fig. 3B), and of the driver genes (Fig. S2). Gene sets obtained from the MSEA analysis were used to perform a GO term enrichment analysis. Significantly enriched pathways included acute-phase response (p=1.01x10^{-8}), acute inflammatory response (p=1.01x10^{-8}), fatty acid beta-oxidation (p=7.43x10^{-5}), fatty acid catabolic process (p=8.99x10^{-4}), cellular lipid catabolic process (p=3x10^{-3}), ion transport (p=3x10^{-2}), cell surface receptor signaling pathway (p=4x10^{-2}), among others associated with biological processes (Fig. 4A). Cellular component analysis highlighted blood

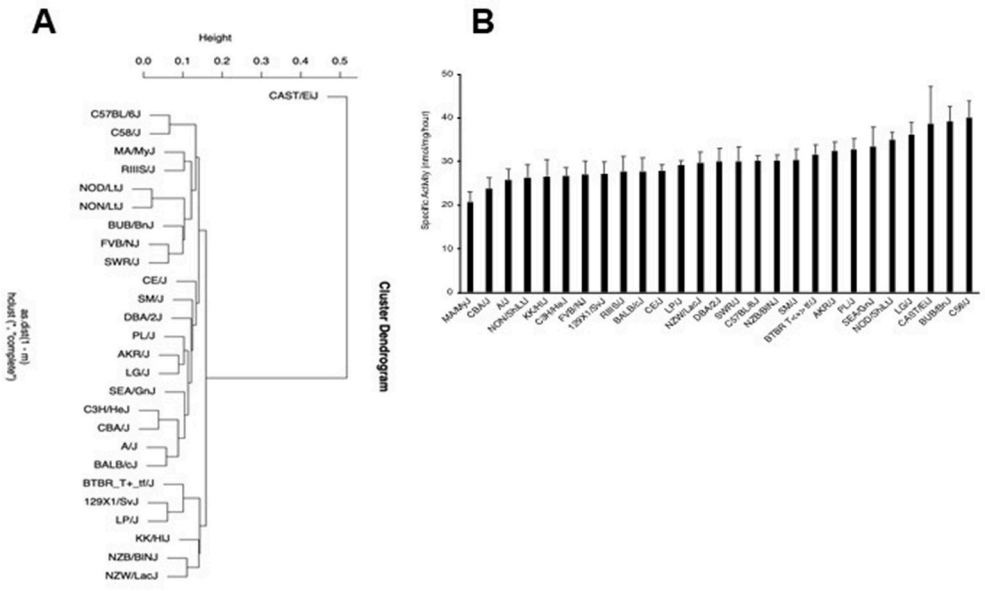

Fig. 1. Variation in the hepatic GCase activity among inbred mouse strains.
(A) Hierarchical clustering of the genetic distance among the 27 used strains, based on EMMA's kinship calculation
(B) Levels of GCase activity in the liver of 27 mouse inbred strains. Values are presented as mean ± standard error (n=5 biological sample with three technical replicates). ANOVA analysis revealed significant differences among the groups (p=0.0028).

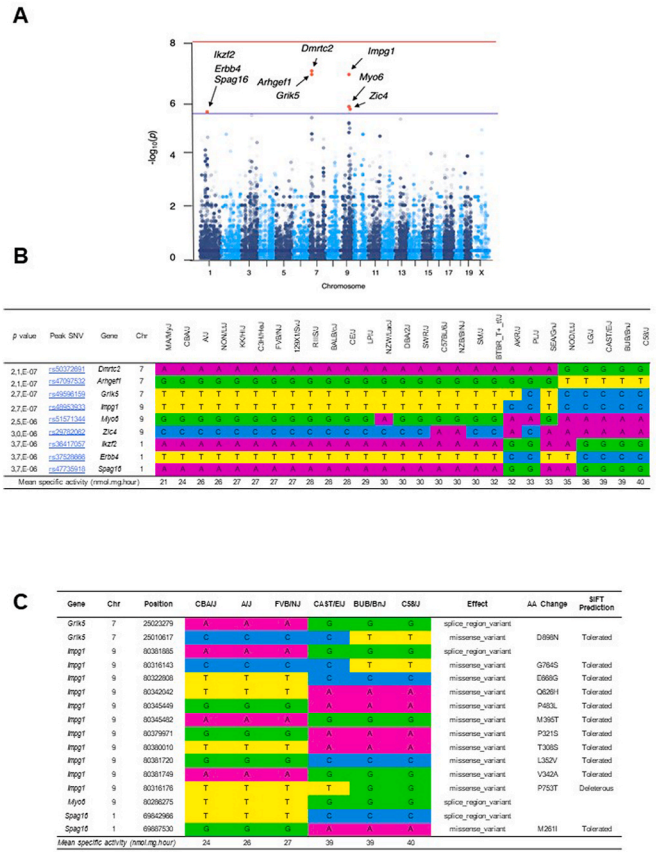

Fig. 2. GWAS identifies putative modifiers of hepatic GCase activity.
(A) Manhattan plot highlights the top associated GCaase activity genes plotted as chromosome position versus the inverse of the negative logarithm of the association p-value.
(B) Strains were organized according to GCase enzymatic activity, from lowest to highest, and the genotype of the peak associated SNV and genomic regions are shown. Adenine (A), purple; cytosine (C), blue; guanine (G), green; thymine (T), yellow; Chr, chromosome.
(C) Miss sense and coding variants in the top associated genes in three strains with low GCase activity and three high activity levels. Same color code than in (B) was used. The effect of the variant, Amino Acid (AA) change, and SIFT prediction were plotted. (For interpretation of the references to color in this figure legend, the reader is referred to the Web version of this article.)

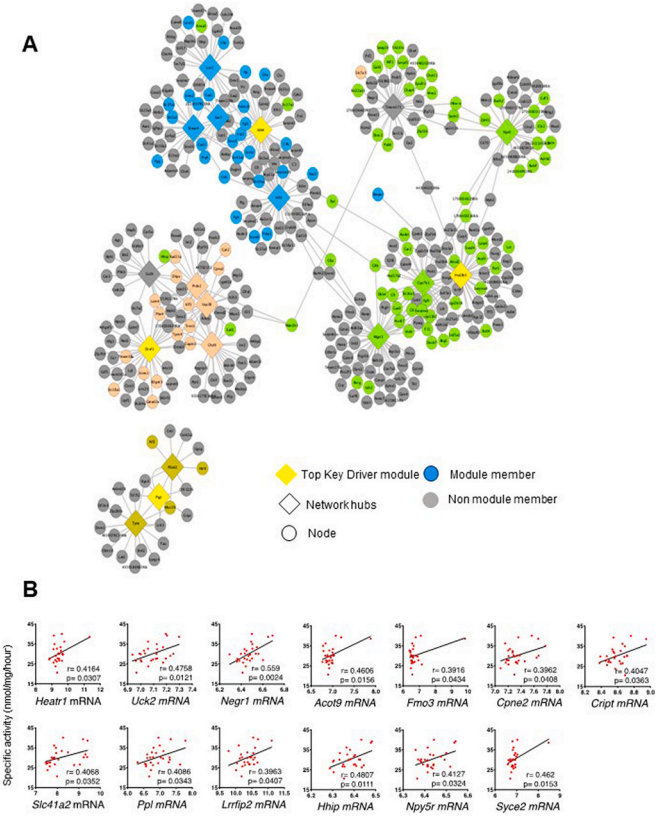

Fig. 3. Integrative network of GCase activity. The gene hubs of the network are represented with diamonds and Key Driver (KD) genes by yellow diamonds. Gene modules are indicated with a different color. Non-member genes are expressed in grey. Red edges show the multiple interactions of KD with other genes.
(A) Itih4; Inter-Alpha-Trypsin Inhibitor Heavy Chain 4.
(B) Hsd3b5; hydroxy-delta-5-steroid dehydrogenase, 3 beta- and steroid delta-isomerase 5.
(C) Ocel1; Occludin/ELL Domain Containing 1.
(D) Pigt; Phosphatidylinositol Glycan Anchor Biosynthesis Class T. (For interpretation of the references to color in this figure legend, the reader is referred to the Web version of this article.)

microparticle (p=6x10^{-2}), early endosome (p=4x10^{-1}), protein-lipid complex (p=4x10^{-1}), organelle lumen (p=4x10^{-1}) and others (Fig. 4B). Molecular function revealed fatty-acyl-CoA binding (p=1x10^{-2}), anion-sodium symporter activity (p=1x10^{-2}), among others (Fig. 4C).

4. Discussion

Our goal was to identify putative modifier genes/networks of hepatic GCase activity using a system genetics strategy. Identifying modulable genetic modifiers of GCase activity offers a feasible and attractive therapeutic alternative for diseases with lysosomal dysfunction, bringing us closer to a precision medicine-based approach.

Our study associated 271 SNVs (Table S1) within nine genes (*Dmrtc2, Arhgef1, Grik5, Impg1, Myo6, Zic4, Ikzf2, Erbb4, Spag16*) to liver GCase activity (Fig. 2A & B), and four key drivers (*Itih4, Hsd3b5, Ocel1, Pigt*) (Fig. 3A-D, Table S3). We found no literature linking these newly associated genes to the GCase enzyme directly. However, the identified genes are associated with several human diseases: *Grik5* to bipolar disorder [30]; *Erbb4* to schizophrenia [31]; and melanoma [32]; *Myo6* to deafness [33]; *Arhgef1* to primary Immunodeficiencies [34]; *Impg1* to vitelliform macular dystrophies [35] and *Zic4* to Dandy-Walker malformation [36]. A connection between these disorders and GCase activity should be therefore be explored.

In addition, the integrative networks identified additional putative regulators of GCase activity. The KD genes have been linked to different functions: *Itih4* to inflammatory responses [37] and liver development and regeneration [38]. *Hsd3b5* to steroid hormones biosynthesis [39], *Ocel1* to cancer prognosis [40] and *Pigt* to glycosylphosphatidylinositol transfer (GPI) proteins [41]. Alterations in these functions have been reported in GD patients, such as i) lymphoid neoplasms [42]; ii) gammopathies [43]; iii) predisposition to infections [44]; iv) immune system dysregulation [45]. Widespread inflammation has been studied in depth in GD. Foamy GD macrophages, known as Gaucher cells, release inflammatory molecules including IL1β, TNF-α, MCP-1 and IL-6, [46,47]. Our results support a role for GCase in the immune response and or this inflammatory pathway(s) can regulate GCase activity.

Our study has some limitations, i) we used public data from a liver expression array of HMDP strains instead of RNAseq. The array has limited probes to capture the transcriptomic landscape of the tissue. Thus, we cannot infer the eventual roles of other genes, different isoforms, splice variants, and genes with a low level of expression [48]. ii) we used liver homogenates. Several cell types make up the liver, and each cell subgroup could have specific contributions to the variability of

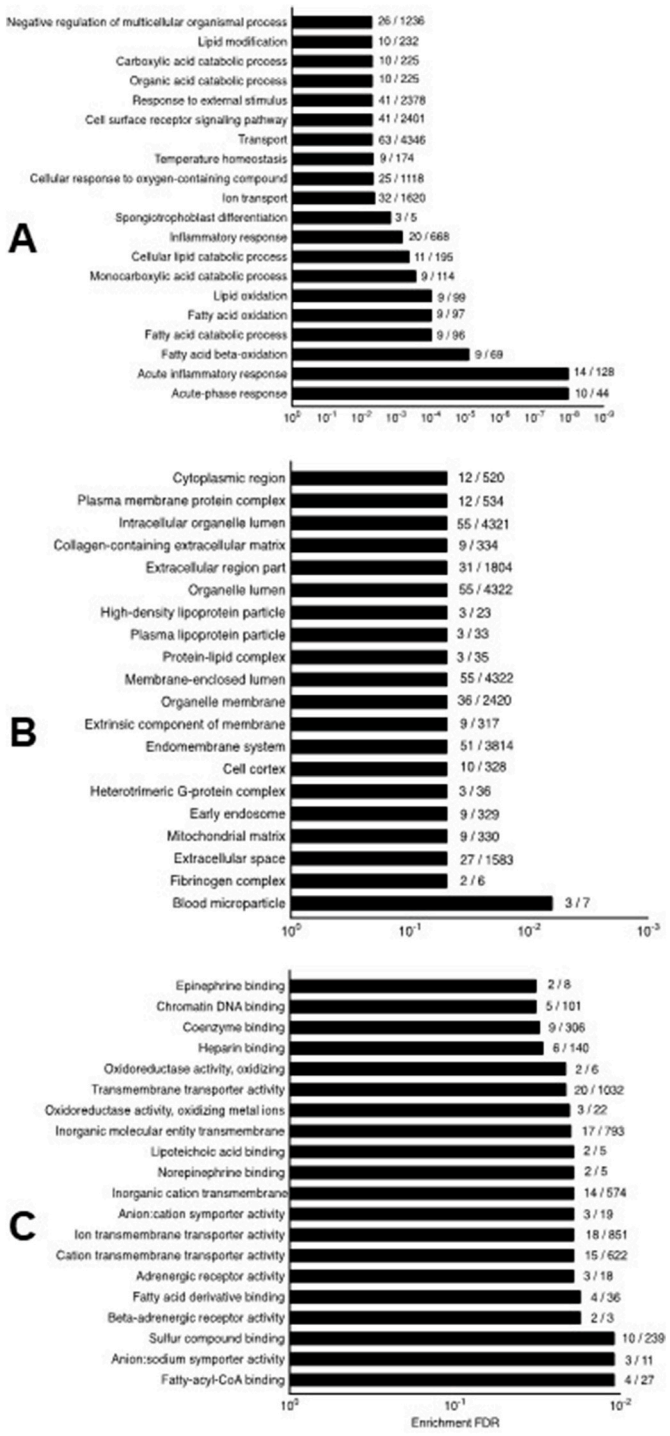

Fig. 4. Identification of enriched GO terms associated with the modules of GCase activity. (A) Biological process. **(B)** Cellular component. **(C)** Molecular function.

the phenotype studied [49–52].

In conclusion, our study has revealed candidate modulators of GCase activity. Further functional analyses are required to understand how the identified genes regulate GCase activity in hepatic cells. The newly identified targets might be relevant for designing therapies for patients with GCase dysfunction, such as Gaucher and Parkinson's disease.

Funding

This work was supported by ANID-CHILE: Fondecyt grant No 1180337 (ADK) (2018–2022) and 1190334 (2019–2023) (SZ), Lyso-Mod, funded by the European Union's Horizon 2020 research and innovation programme (RISE) under the Marie Sklodowska-Curie grant agreement No 734825 (SZ, FMP, ADK) (2017–2022), and the Mizutani Foundation for Glycoscience, grant No: 200133 (FMP, DAP, ADK) (2020). Funding for computational infrastructure was provided by FONDEQUIP EQM150093. FP is a Wolson Royal Society Merit Award Holder and a Wellcome Trust Investigator in science.

Author contributions

AD, BRJ, and DAP performed the experiments, analyzed the data, wrote the paper. VO, and JFC reviewed and edited the document and provided helpful discussions. ADK, SZ, FMP conceptualization, analyzed the data, revised the manuscript, funding acquisition.

Declaration of competing interest

None.

Acknowledgments

The authors acknowledge Dr. Aldons Lusis (University of California, Los Angeles) for kindly donating mouse livers.

Appendix A. Supplementary data

Supplementary data to this article can be found online at https://doi.org/10.1016/j.bbrep.2021.101105.

References

[1] T. Lübke, P. Lobel, D.E. Sleat, Proteomics of the lysosome, Biochim. Biophys. Acta Mol. Cell Res. 1793 (2009) 625–635, https://doi.org/10.1016/j.bbamcr.2008.09.018.
[2] A. Ballabio, J.S. Bonifacino, Lysosomes as dynamic regulators of cell and organismal homeostasis, Nat. Rev. Mol. Cell Biol. 21 (2020) 101–118, https://doi.org/10.1038/s41580-019-0185-4.
[3] R.O. Brady, J.N. Kanfer, R.M. Bradley, et al., Demonstration of a deficiency of glucocerebroside-cleaving enzyme in Gaucher's disease, J. Clin. Invest. 45 (1966), https://doi.org/10.1172/JCI105417.
[4] J.F. Desforges, E. Beutler, Gaucher's disease, N. Engl. J. Med. 325 (1991), https://doi.org/10.1056/NEJM199111073251906.
[5] E. Sidransky, M.A. Nalls, J.O. Aasly, et al., Multicenter analysis of glucocerebrosidase mutations in Parkinson's disease, N. Engl. J. Med. (2009) 361, https://doi.org/10.1056/NEJMoa0901281.
[6] A.D. Klein, J.R. Mazzulli, Is Parkinson's disease a lysosomal disorder? Brain 141 (2018) 2255–2262, https://doi.org/10.1093/brain/awy147.
[7] R. Giugliani, F. Vairo, F. Kubaski, et al., Neurological manifestations of lysosomal disorders and emerging therapies targeting the CNS, Lancet Child Adolescent Health 2 (2018) 56–68, https://doi.org/10.1016/S2352-4642(17)30087-1.
[8] A. Ghazalpour, C.D. Rau, C.R. Farber, et al., Hybrid mouse diversity panel: a panel of inbred mouse strains suitable for analysis of complex genetic traits, Mamm. Genome 23 (2012) 680–692, https://doi.org/10.1007/s00335-012-9411-5.
[9] A.D. Klein, Modeling diseases in multiple mouse strains for precision medicine studies, Physiol. Genom. 49 (2017) 177–179, https://doi.org/10.1152/physiolgenomics.00123.
[10] M. Civelek, A.J. Lusis, Systems genetics approaches to understand complex traits, Nat. Rev. Genet. 15 (2014) 34–48, https://doi.org/10.1038/nrg3575.
[11] J. Flint, E. Eskin, Genome-wide association studies in mice, Nat. Rev. Genet. 13 (2012) 807–817, https://doi.org/10.1038/nrg3335.
[12] A.J. Lusis, M. Seldin, H. Allayee, et al., The Hybrid Mouse Diversity Panel: A Resource for Systems Genetics Analyses of Metabolic and Cardiovascular Traits, 2016. www.jlr.org.
[13] A.D. Klein, N.S. Ferreira, S. Ben-Dor, . J, et al., Identification of modifier genes in a mouse model of gaucher disease, Cell Rep. 16 (2016) 2546–2553, https://doi.org/10.1016/j.celrep.2016.07.085.
[14] R.J. Ferland, J. Smith, D. Papandrea, et al., Multidimensional genetic analysis of repeated seizures in the hybrid mouse diversity panel reveals a novel epileptogenesis susceptibility locus, G3: genes, Genomes, Genetics, 7, https://doi.org/10.1534/g3.117.042234, 2017, 2545-2558.

[15] D. Robinson, The fluorimetric determination of β-glucosidase: its occurrence in the tissues of animals, including insects, Biochem. J. 63 (1956), https://doi.org/10.1042/bj0630039.
[16] S. van Weely, M. Brandsma, A. Strijland, J.M. Tager, J.M.F.G. Aerts, Demonstration of the existence of a second, non-lysosomal glucocerebrosidase that is not deficient in Gaucher disease, Biochim. Biophys. Acta (BBA) - Mol. Basis Dis. (1993) 1181, https://doi.org/10.1016/0925-4439(93)90090-N.
[17] M.K. Hyun, N.A. Zaitlen, C.M. Wade, A, et al., Efficient control of population structure in model organism association mapping, Genetics 178 (2008) 1709–1723, https://doi.org/10.1534/genetics.107.080101.
[18] A. Kirby, H.M. Kang, C.M. Wade, C, et al., Fine mapping in 94 inbred mouse strains using a high-density haplotype resource, Genetics 185 (2010) 1081–1095, https://doi.org/10.1534/genetics.110.115014.
[19] R. R Core Team, A Language and Environment for Statistical Computing, R Foundation for Statistical Computing, 2020, 1–1.
[20] B.J. Bennett, C.R. Farber, L. Orozco, et al., A high-resolution association mapping panel for the dissection of complex traits in mice, Genome Res. 20 (2010) 281–290, https://doi.org/10.1101/gr.099234.109.
[21] D.J. Adams, A.G. Doran, Lilue, et al., The Mouse Genomes Project: a repository of inbred laboratory mouse strain genomes, Mamm. Genome 26 (9–10) (2015) 403–412, https://doi.org/10.1007/s00335-015-9579-6.
[22] R. Vaser, S. Adusumalli, S.N. Leng, M. Sikic, et al., SIFT missense predictions for genomes, Nat. Protoc. 11 (1) (2015) 1–9, https://doi.org/10.1038/nprot.2015.123.
[23] P. Cingolani, A. Platts, L.L. Wang, Coon, et al., A program for annotating and predicting the effects of single nucleotide polymorphisms, SnpEff. Fly 6 (2) (2012) 80–92, https://doi.org/10.4161/fly.19695.
[24] D. Arneson, A. Bhattacharya, L. Shu, et al., Mergeomics: a web server for identifying pathological pathways, networks, and key regulators via multidimensional data integration, BMC Genom. 17 (2016), https://doi.org/10.1186/s12864-016-3057-8.
[25] P. Langfelder, S. Horvath, WGCNA: an R package for weighted correlation network analysis, BMC Bioinf. 9 (2008), https://doi.org/10.1186/1471-2105-9-559.
[26] Y. Benjamini, Y. Hochberg, Controlling the false discovery rate: a practical and powerful approach to multiple testing, J. Roy. Stat. Soc. B 57 (1995) 289–300.
[27] S.S. Wang, E.E. Schadt, H. Wang, et al., Identification of pathways for atherosclerosis in mice: integration of quantitative trait locus analysis and global gene expression data, Circ. Res. 101 (2007), https://doi.org/10.1161/CIRCRESAHA.107.152975.
[28] S.X. Ge, D. Jung, R. Yao, ShinyGO: a graphical gene-set enrichment tool for animals and plants, Bioinformatics 36 (2020), https://doi.org/10.1093/bioinformatics/btz931.
[29] J. Chebib, B.C. Jackson, E. López-Cortegano, et al., Inbred lab mice are not isogenic: genetic variation within inbred strains used to infer the mutation rate per nucleotide site, Heredity 126 (2021) 107–116, https://doi.org/10.1038/s41437-020-00361-1.
[30] M. Beneyto, L.v. Kristiansen, A. Oni-Orisan, R.E. McCullumsmith, J.H. Meador-Woodruff, Abnormal glutamate receptor expression in the medial temporal lobe in schizophrenia and mood disorders, Neuropsychopharmacology 32 (2007) 1888–1902, https://doi.org/10.1038/sj.npp.1301312.
[31] C.G. Hahn, H.Y. Wang, D.S. Cho, et al., Altered neuregulin 1-erbB4 signaling contributes to NMDA receptor hypofunction in schizophrenia, Nat. Med. 12 (2006) 824–828, https://doi.org/10.1038/nm1418.
[32] T.D. Prickett, N.S. Agrawal, X. Wei, et al., Analysis of the tyrosine kinome in melanoma reveals recurrent mutations in ERBB4, Nat. Genet. 41 (2009), https://doi.org/10.1038/ng.438.
[33] Z.M. Ahmed, R.J. Morell, S. Riazuddin, A, et al., Mutations of MYO6 are associated with recessive deafness, DFNB37, Am. J. Hum. Genet. (2003) 72, https://doi.org/10.1086/375122.
[34] A. Bouafia, S. Lofek, J. Bruneau, L, et al., Loss of ARHGEF1 causes a human primary antibody deficiency, J. Clin. Invest. 129 (2019) 1047–1060, https://doi.org/10.1172/JCI120572.
[35] G. Manes, I. Meunier, A. Avila-Fernández, et al., Mutations in IMPG1 cause vitelliform macular dystrophies, Am. J. Hum. Genet. 93 (2013) 571–578, https://doi.org/10.1016/j.ajhg.2013.07.018.
[36] I. Grinberg, H. Northrup, H. Ardinger, C, et al., Heterozygous deletion of the linked genes ZIC1 and ZIC4 is involved in Dandy-Walker malformation, Nat. Genet. 36 (2004) 1053–1055, https://doi.org/10.1038/ng1420.
[37] Y. Ma, R. Li, J. Wang, et al., ITIH4, as an inflammation biomarker, mainly increases in bacterial bloodstream infection, Cytokine 138 (2021), https://doi.org/10.1016/j.cyto.2020.155377.
[38] C.D. Bhanumathy, Y. Tang, S.P.S. Monga, et al., Itih-4, a serine protease inhibitor regulated in interleukin-6-dependent liver formation: role in liver development and regeneration, Dev. Dynam. 223 (2002) 59–69, https://doi.org/10.1002/dvdy.1235.
[39] C. Park, Expression of multiple forms of 3β-hydroxysteroid dehydrogenase in the mouse liver during fetal and postnatal development, Mol. Cell. Endocrinol. 116 (1996), https://doi.org/10.1016/0303-7207(95)03707-1.
[40] M. Deng, Z. Zhang, B. Liu, et al., Low OCEL1 expression is associated with poor prognosis in human non-small cell lung cancer, Canc. Biomarkers 27 (2020) 519–524, https://doi.org/10.3233/CBM-191268.
[41] K. Ohishi, PIG-S and PIG-T, essential for GPI anchor attachment to proteins, form a complex with GAA1 and GPI8, EMBO J. 20 (2001), https://doi.org/10.1093/emboj/20.15.4088.
[42] B.E. Rosenbloom, N.J. Weinreb, A. Zimran, et al., Gaucher disease and cancer incidence: a study from the Gaucher Registry, Blood 105 (2005) 4569–4572, https://doi.org/10.1182/blood-2004-12-4672.
[43] Y. Nguyen, J. Stirnemann, F. Lautredoux, et al., Immunoglobulin abnormalities in Gaucher disease: an analysis of 278 patients included in the French gaucher disease registry, Int. J. Mol. Sci. 21 (2020), https://doi.org/10.3390/ijms21041247.
[44] L. Marodi, R. Kaposzta, J. Toth, A, et al., Impaired microbicidal capacity of mononuclear phagocytes from patients with type I Gaucher disease: partial correction by enzyme replacement therapy, Blood 86 (1995), https://doi.org/10.1182/blood.V86.12.4645.bloodjournal86124645.
[45] M.K. Pandey, T.A. Burrow, R. Rani, et al., Complement drives glucosylceramide accumulation and tissue inflammation in Gaucher disease, Nature 543 (2017) 108–112, https://doi.org/10.1038/nature21368.
[46] D.M. Mosser, J.P. Edwards, Exploring the full spectrum of macrophage activation, Nat. Rev. Immunol. 8 (2008) 958–969, https://doi.org/10.1038/nri2448.
[47] A. Mantovani, A. Sica, S. Sozzani, P, et al., The chemokine system in diverse forms of macrophage activation and polarization, Trends Immunol. 25 (2004) 677–686, https://doi.org/10.1016/j.it.2004.09.015.
[48] P. Uciechowski, W.C.M. Dempke, Interleukin-6: a masterplayer in the cytokine network, Oncology (Switzerland) 98 (2020) 131–137, https://doi.org/10.1159/000505099.
[49] S. Zhao, W.P. Fung-Leung, A. Bittner, et al., Comparison of RNA-Seq and microarray in transcriptome profiling of activated T cells, PloS One 9 (2014), https://doi.org/10.1371/journal.pone.0078644.
[50] S.A. MacParland, J.C. Liu, X.Z. Ma, et al., Single cell RNA sequencing of human liver reveals distinct intrahepatic macrophage populations, Nat. Commun. 9 (2018), https://doi.org/10.1038/s41467-018-06318-7.
[51] N. Aizarani, A. Saviano, Sagar, et al., A human liver cell atlas reveals heterogeneity and epithelial progenitors, Nature 572 (2019) 199–204, https://doi.org/10.1038/s41586-019-1373-2.
[52] X. Wang, L. Yang, Y.C. Wang, et al., Comparative analysis of cell lineage differentiation during hepatogenesis in humans and mice at the single-cell transcriptome level, Cell Res. 30 (2020) 1109–1126, https://doi.org/10.1038/s41422-020-0378-6.